

ALTERED RHYOLITIC ROCKS IN THE VISÉ BOREHOLES: A GEOCHEMICAL APPROACH

Jean-Clair DUCHESNE¹, Eric GOEMAERE², Jean-Christophe GRIGOLATO¹, Hyacinthe VANDERSCHUEREN³ & Bernard CHARLIER¹

(13 figures, 1 plate, 4 tables)

1. *Unité de recherches de Pétrologie et Géochimie endogènes, Département de Géologie, B20, Université de Liège, B-4000 SART TILMAN (Belgique); e-mail: jc.duchesne@ulg.ac.be*

2. *Service géologique de Belgique, Institut Royal des Sciences Naturelles de Belgique, 13, rue Jenner, 1050 BRUXELLES (Belgique)*

3. *Service de mesure et instrumentation électriques, Institut d'Electricité Montefiore, B28, Université de Liège, B-4000 SART TILMAN (Belgique)*

ABSTRACT. Under a sedimentary cover of calcareous breccias of Dinantian and Frasnian ages, and a conglomeratic level with volcanic clasts, a magmatic rock, presumably belonging to the Ordovician-Silurian magmatic province, was cut across in two boreholes at Visé (Quarry K). Macroscopically the rock is brecciated and locally displays evidence of flow structures. Microscopically, it shows various stages of alteration (devitrification, silicification, carbonation and sericitation) superimposed on magmatic flow structures, the most evolved assemblage being quartz + illite ± sulphides ± carbonates. 27 whole-rock analyses (major and trace elements by XRF) show large ranges of chemical variations, e.g. 51 to 80% SiO₂, 1.7 to 10% K₂O, 0.03 to 6.6% Na₂O, making impossible the use of classical petrochemical methods of identification. In the classic AFC-AKF projections of Eskola, the most altered rocks appear made up of various proportions of quartz and an illite of restricted composition. This clay mineral is similar in composition to hydrothermal illite from the phyllic alteration of the Bingham porphyry copper deposit and from the Los Azufres volcanic centre. This points to identical conditions of formation ca. 310°C. Although the original magmatic rock has been deeply metasomatised by addition and subtraction of mobile elements, the ratios of some trace elements, such as Zr, Nb, Y, Th, REE and Ti, have been preserved, thus confirming that these elements were immobile during the alteration processes. It is therefore possible to use their ratios to identify the nature of the protolith by means of the Winchester and Floyd (1977) discrimination diagram. It turns out that the Visé felsic rock protolith is effectively a rhyolite. Multi-element diagrams also point to calc-alkaline series of rock, with « Within Plate Granite » characteristics. This suggests a formation in a post-collisional extensional environment. Interestingly, analysis of 2 samples from the conglomeratic level above the unconformity shows that the volcanic clastic material has a different immobile element signature than the rhyolite. Thus it could have its origin in another volcanic rock, Ordovician-Silurian or Devonian in age.

KEYWORDS: rhyolites, Visé, Brabant Massif, phyllic alteration, berezite, metasomatism, immobile elements.

1. Introduction

In 1987, the Geological Survey of Belgium drilled the northern part of the K-L quarry, by the Argenteau-Visé road, in eastern Belgium. This quarry is in the Souvré block, in the central part of a previously described dome structure (Poty, 1991). A first drill core, called Visé 1 (V1), was performed to document the structural and sedimentological characteristics of the Paleozoic rocks of the area and to check the possible occurrence of Cambro-Silurian rocks in the lower part of the dome structure. Below some 200 m of Paleozoic sedimentary rocks, the borehole intercepted siliceous rocks of volcanic origin (Poty, 1991). The rocks were macroscopically identified as metarhyolites, locally extremely altered (Goemaere & Vandeven, 1989). An incident imposed stopping the drilling at 241,7 m depth. A second drill core was then executed, some ten meters from the first one, in order to reach the base of these volcanic rocks. This second borehole, named Visé 1bis (V1b), reached a depth of 329,5 m but did not cut across the base of the rhyolites. One can thus only give a

minimal estimate of the age of these volcanic rocks: as Frasnian to Givetian limestones overlie them, they must be older than the latter. A maximum Cambro-Silurian age can possibly be inferred because Visé is situated in the prolongation of the volcanic arc which has bordered the south part of the Brabant Massif, a zone marked by extrusive magmatism including lavas, ignimbrites, breccias and tuffs of rhyolitic to dacitic composition and ranging from upper Ordovician to middle Silurian (André *et al.*, 1986; André, 1991).

We have studied the petrography and geochemistry of these igneous rocks in order better to define their nature and to compare them with known occurrences of similar rocks in Belgium. A series of samples have been analysed for major and trace elements, including Radon, to specify the geochemistry of these rocks, which are marked by a deep hydrothermal alteration. We will also document the mineralogical characteristics of the metasomatic alteration and define the temperature conditions at which it has developed. The immobile character of some elements will be ascertained in order

to allow the identification of the rock type and geodynamic setting.

2. Geological setting

During the upper Ordovician, the Brabant Massif (Fig. 1) belonged to the Avalonia microcontinent and formed with East Anglia a 420 km-long and 120 km-wide subsident foreland basin (Van Grootel *et al.*, 1997; Verniers *et al.*, 2002). The south margin of the Brabant Massif was affected by a calc-alkaline subduction-related magmatism resulting from the partial melting of the Tornquist oceanic lithosphere subducted under Avalonia (André *et al.*, 1986; Pharaoh *et al.*, 1993). By means of microfossils from sediments interbedded with the volcanic units, the volcanism is dated from the Ashgillian to the Wenlock, and the ages differed from E to W: Ashgillian in the western part, Caradocian in the central part and Wenlockian in the eastern part (André, 1991).

Subduction was followed by collision, which resulted in folding, cleavage development and thrusting during the mid-Lochkovian to mid-Eifelian (Acadian deformation). This deformation produced basin inversion and the regional antiform structure of the Brabant Massif (see the review by Van Grootel *et al.*, 1997). A low grade metamorphism (anchizone to mesozone) has affected the whole area.

In the Visé-Maastricht area, the eastern part of the Brabant Massif is concealed below Paleozoic sediments. Its post-Caledonian tectono-sedimentary history is complex and controlled by block-faulting during the Devonian and the Carboniferous (Poty, 1991).

3. Petrography and mineralogy

3.1. Drill cores description and sample location

The two drill cores (V1 and V1b) were first described by Goemaere & Vandeven (1989). The lithologies intercepted by the drill core are lower Viséan sedimentary breccias lying on a few meters of pelites (probably dating from Upper Frasnian), limestones breccias with Middle Frasnian clasts from the Lustin Formation, conglomerates most likely of Frasnian or Givetian age, and, finally, below an unconformity, felsic igneous rocks (Poty, 1991). The unconformity is located at 202 m in V1 and at 228 m in V1b, the offset resulting from a normal fault between the two boreholes. The conglomeratic rocks, 20 m thick, just above the unconformity, are polygenic conglomerates with a significant proportion of angular volcanic clasts. Two of our samples (analyses n° 1 and 2) were taken from this unit, the rest of the samples representing the felsic igneous rock below the unconformity at depths indicated in Table 1. The petrographic description is based on macroscopic textures and on thin sections.

3.2 Petrography

A thorough petrographic interpretation of the rocks is outside the scope of the present paper. The rocks have indeed been deeply altered by a variety of processes. The primary igneous textures of the felsic rock are totally blurred: porphyritic minerals, typical of acidic volcanics, such as feldspar euhedral phenocrysts or rounded embayed quartz have not been observed; glass shards, perlitic fractures, etc. are absent. The only still identifiable volcanic texture has been found in an angular clast in a pyroclastic breccia (Plate 1, ph. F), which points to different source material and degree of alteration. Although the result of the alteration of the Visé felsic

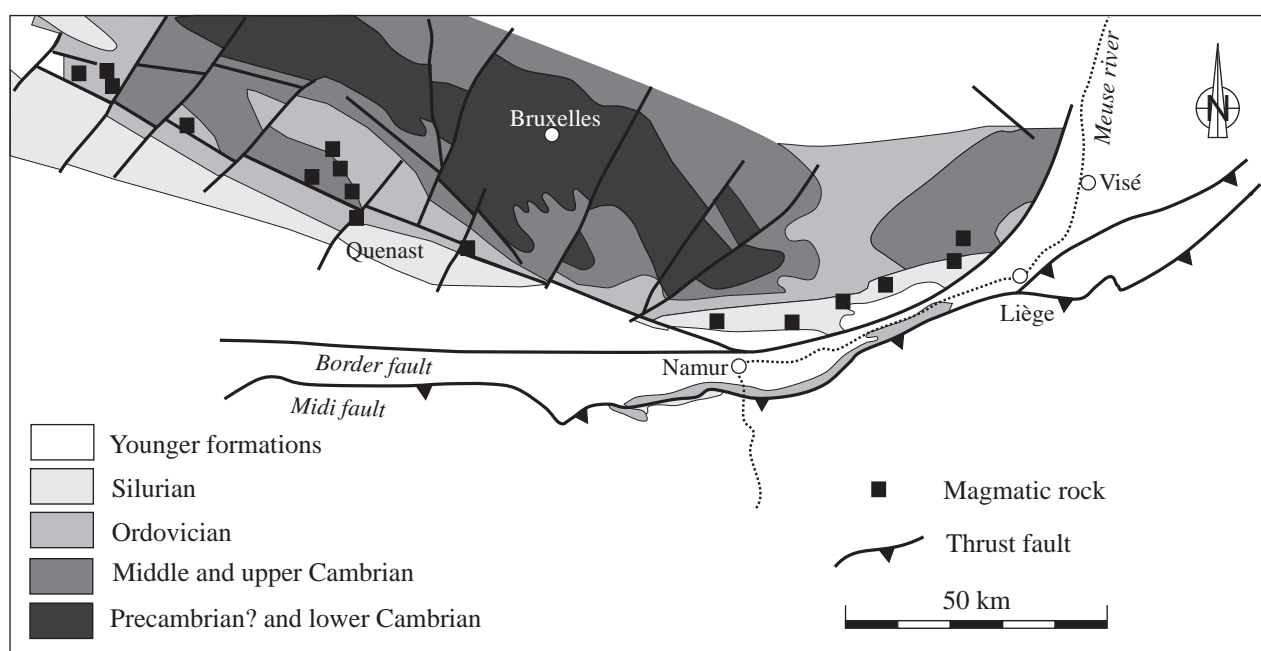


Fig. 1 : Subcrop geological map of the Brabant Massif (after De Vos *et al.*, 1993, and Chacksfield *et al.*, 1993).

rock is difficult to interpret in detail, a few points are worth mentioning.

The Visé felsic rock is rarely massive and often brecciated, with veins, cracks and fractures cutting out the rock (Plate 1, ph. A). Several mechanisms can explain the origin of the volcanic breccias (see the review by McPhie *et al.*, 1993). They can be regarded as hyaloclastites, which are aggregates of clasts formed by non-explosive fragmentation and disintegration, induced by rapid cooling of the external envelope of a lava flow (autobrecciation). Breccia could also have a pyroclastic origin when it is polygenic (Plate 1, ph. F). Finally, some lithological units show secondary brecciation superimposed on an initial breccia. Cement of this secondary brecciation is frequently quartz and spathic calcite. Other identifiable macroscopic textures are characteristic of extrusive volcanic rocks. Flow foliation (McPhie *et al.*, 1993) is revealed by various textures, such as vermiculated, ribboned, folded, stretched, and convolute textures (Plate 1, ph. B to D). All those were created by plastic deformation (creep) of the rock before complete solidification. Many vesicles and amygdales (vesicles filled by secondary minerals) are also present and were mainly generated at the time of fluid exsolution by the magma.

Microscopic textures confirm the extrusive volcanic origin and the glassy nature of the studied felsic rocks. Various textures due to devitrification are visible (Vernon, 2004): spherulites (Plate 1, ph. G), crested quartz rim (Plate 1, ph. E and H), and a variety of quartz crystals at different stages of recrystallization (Plate 1, ph. E). The rocks are also affected by various alteration processes: illitisation (Plate 1, ph. C-D), carbonatation, and silicification.

3.3. Mineralogy

The resulting mineralogy of the felsic rock is very simple. It is mainly made up of quartz, illite (or sericite), carbonate, sulphides and various amounts of altered feldspars. Chlorite and biotite are absent. Illite can sometimes completely replace the original rock while preserving the macroscopic texture of the rock, such as flow banding (Plate 1, ph. B-D). Spathic calcite can also be present in vein. Euhedral pyrite grains are ubiquitous and sphalerite can be locally present (XRD determination).

The clay mineralogy was studied by XRD (see the Appendix). Illite (1M polymorph) is the only clay mineral present. Following Esquevin (1969), the 5 Å/10 Å peak intensity ratio is an indicator of the illite chemistry (cations in the octahedral sheet). The measured values (7 samples) are >0.40 (0.4 to 0.6), indicative of Al-rich illites (muscovite and sericite). The small asymmetry to the low-angle side of the 10 Å XRD peak indicates a slightly open illite. The Kübler illite crystallinity index varies between 0.33 and 0.40, which corresponds to the highest grade of low-grade metamorphism and to hydrothermal illites (see the review by Parry *et al.*, 2002). The intensity ratio “Ir” for illites (Ir = I(001)/I(003) air dried)/I(001)/I(003) glycolated) varies between 1.089 and 1.146 (in samples where quartz interference is minimum) and indicates 1 to 2 percent of expandable layers in illite. A chemical analysis of an

Analysis #	1	2	3	4	5	6	7	8	9	10	11	12	13	14	15	16	17	18	19	20	21	22	23	24	25	26	27	28	29	30	
Sample #	V1-09	V1-10	V1-13	V1-14	V1-15	V1-16	V1-17	V1-18	V1-19	V1-4	V1-5	V1-6	V1-7	V1-8	V1-9	V1-13	V1-33	V1-50	V1-61	V1-71	V1-74	V1-79	V1-85	V1-53	V1-65	V1-70	V1-78	V1-8V	RV (3)	B Tuff	
Depth (m)	192.0	193.4	220.1	211.1	205.0	205.8	209.1	220.8	227.0	232.7	263.9	269.0	289.0	321.0	325.0	234.9	259.2	277.1	285.7	292.2	299.0	309.9	247.8	288.9	292.2	307.3	269	269	269		
Major elements (%)																															
SiO2	66.02	62.22	75.99	82.92	75.46	68.99	60.54	76.67	78.16	76.84	81.86	54.67	75.33	65.25	69.31	70.98	65.90	72.40	80.30	79.43	53.06	76.33	51.52	76.81	75.83	80.25	80.33	50.59	53.69	77.40	
TiO2	0.93	0.44	0.31	0.16	0.23	0.35	0.60	0.25	0.20	0.22	0.16	0.63	0.27	0.15	0.26	0.39	0.30	0.21	0.18	0.18	0.67	0.20	0.79	0.20	0.26	0.17	0.18	0.61	0.65	0.07	
Al2O3	17.08	9.21	13.43	9.09	13.19	17.94	22.29	12.26	10.27	12.72	8.33	27.97	14.80	8.60	14.69	17.67	18.30	12.29	9.65	10.45	27.35	11.64	28.08	13.38	13.71	10.35	10.73	26.86	28.51	12.30	
FeOtot	6.61	4.92	1.19	0.42	1.50	2.87	4.08	0.60	0.81	0.49	0.40	3.48	2.28	2.77	1.51	1.16	0.38	0.46	0.97	1.21	3.01	1.93	3.48	0.95	2.55	1.12	0.69	3.36	3.57	0.70	
MnO	0.02	7.01	0.01	0.01	0.63	0.01	0.01	0.06	0.02	0.01	0.02	0.16	0.01	0.09	0.06	0.01	0.01	0.02	0.02	0.02	0.01	0.03	0.01	0.02	0.01	0.01	0.01	0.01	0.01	0.01	
MgO	1.11	0.27	0.39	0.06	0.01	1.17	1.60	0.01	0.86	0.10	0.51	0.01	1.19	1.76	2.42	1.18	0.22	0.86	0.24	0.03	2.35	0.01	2.68	0.09	1.11	0.05	0.03	2.95	3.13	0.01	
CaO	0.36	12.41	0.06	0.39	2.42	0.86	0.55	0.10	1.55	0.09	1.66	0.08	0.34	15.12	4.31	0.84	0.82	2.20	0.64	0.02	0.86	0.03	1.07	0.24	0.05	0.11	0.05	0.14	0.15	0.45	
Na2O	0.03	0.06	0.30	2.19	2.51	1.09	0.38	0.37	1.19	2.92	1.05	0.05	0.17	2.81	3.00	1.30	4.54	2.70	3.02	4.24	0.09	6.62	0.18	5.54	0.07	4.43	6.15	0.06	0.06	3.90	
K2O	5.69	2.95	7.98	3.73	2.99	5.46	7.45	9.52	5.72	5.67	5.23	10.11	5.31	1.75	3.64	5.77	8.68	7.17	3.64	2.52	10.23	2.97	10.44	3.85	5.07	2.40	2.42	9.65	10.24	4.80	
P2O5	0.09	0.09	0.06	0.02	0.03	0.04	0.05	0.03	0.03	0.02	0.02	0.05	0.03	0.02	0.03	0.03	0.06	0.03	0.03	0.02	0.06	0.03	0.07	0.05	0.03	0.03	0.03	0.03	0.01	0.01	
Sum	98.88	99.58	99.85	99.04	98.97	99.08	98.01	99.87	98.89	99.13	99.29	99.21	99.97	98.63	99.40	99.47	99.19	98.43	98.79	98.26	98.04	100.00	100.00	101.23	98.97	99.04	100.68	100.51(2)	100.00	99.91	
LOI	7.29	15.23	2.49	1.45	4.42	4.87	5.80	1.51	3.39	1.26	2.42	5.83	4.06	12.21	7.35	4.01	1.63	3.59	1.79	1.52	6.07	1.60	7.51	1.25	3.48	1.47	1.22	6.24	6.24	6.24	
Trace elements (ppm)																															
Rb	167	77	144	62	87	166	262	150	93	97	80	405	199	32	95	185	134	113	69	45	429	44	422	56	207	40	40	40	40	190	
Sr	15	46	30	55	84	87	114	39	48	73	43	31	13	110	52	83	123	78	92	44	24	52	19	76	10	45	36	65	65	25	
Y	15	20	89	55	84	87	114	51	86	74	45	156	75	93	83	114	505	321	323	100	57	129	66	152	70	56	65	65	25	25	
Zr	149	107	418	283	422	543	878	378	315	367	260	841	405	244	446	623	505	321	323	100	344	1059	344	1059	343	410	317	387	85	85	
Nb	16	9	19	14	18	23	35	16	15	11	11	36	18	11	19	27	20	15	15	16	34	16	42	16	14	16	14	16	16	22	
Th	13	5	26	20	29	36	56	25	22	24	18	56	28	16	30	43	32	20	23	23	57	24	68	23	29	24	24	24	22	22	
U	7.5	2.7	5.6	7.9	5.4	3.5	5.9	4.8	4.6	7.9	2.8	12.5	2.3	4.6	6.5	4.4	5	2.9	5.9	3.5	3.5	5.9	13.1	6.5	9.2	5.1	6.1	6.5	6.5		
Pb	36	29	19	12	11	21	17	17	14	13	11	16	17	52	24	25	13	12	21	14	22	28	26	12	20	14	14	14	14		
Co	31	20	5	5	0	7	0	0	0	0	0	9	7	4	4	4	9	0	0	3	12	0	13	1	6	4	2	2	2	2	
Cu	27	14	17	6	7	3	3	7	2	3	1	3	4	4	4	4	3	1	0	3	2	0	4	1	6	4	2	2	2	2	
Ga	19	12	39	10	25	39	92	10	12	10	8	65	37	13	43	39	15	10	12	14	92	16	107	11	35	13	15	15	1	1	
Ni	39	25	15	21	26	11	13	9	13	9	9	10	11	12	10	6	5	3	2	2	9	1	13	0	3	2	2	2	2	1	
Zn	12	9	20	8	153	10	17	25	5	15	15	52	238	258	184	11	16	5	14	212	30	152	25	9	52	167	88	88	38	38	
Radon (Bq/m ³ kg)																															
Rn	4.0	8.5	8.5	8.5	7.5	4.9	7.3	6.5	7.3	6.8	4.7	16.1	6.8	3.9	4.4	11.9	5.2	4.4	4.4	4.6	7.3	3.5	17.1	6.4	5.8	5.8	5.8	5.8	5.8	5.8	5.8

(1) name of the borehole (V1 and V1b) followed by sample number; (2) including 4.85% H2O4, 1.2% FeO, and 1.51%Si; (3) RV analysis recalculated on a calculated basis (to permit comparison with the other XRF analyses)

Table 1: Major and trace element compositions of whole-rock samples from the Visé boreholes and of a rhyolite from the Bishop tuff (Hildreth, 1981).

illitic rock (sample V1b.RV) by conventional wet chemistry is reported in Table 1 (analysis n° 28) and XRD powder data are reported in Table 2. After subtracting the composition of normative pyrite (analysis n°29), the structural formula based on 11 oxygen atoms per unit cell has been calculated and is reported in Table 3.

4. Geochemical approach

The petrographic study has shown that the Visé igneous rock has been deeply altered through several processes: devitrification, silicification, carbonatisation and illitisation. The geochemistry of the rocks will thus reflect this complex metasomatic evolution. 27 samples have been selected in massive rocks to avoid as much as possible contamination by crack- and vein-filling material. They were analysed for major and some trace elements by X-ray fluorescence (XRF), and some of them were also analysed for Hf, Ta and REE by ICP-MS, and for Ra, following methods described in the Appendix. S and FeO were also analysed in the illitic sample RV (analysis n°28). Analyses are reported in Table 1 together with the composition of a typical rhyolite from the Bishop Tuff (Hildreth, 1981).

Intensity	I/I ₀	d exp (Å)	hkl
120	100	10.07	001
70	58	5.04	002
118	98	4.51	020
49	41	4.38	11 $\bar{1}$
23	19	4.13	021
95	79	3.67	11 $\bar{2}$
260	+100	3.34	003 & 022
104	87	3.08	112
41	34	2.93	11 $\bar{3}$
37	31	2.69	023
139	+100	2.59/2.57	13 $\bar{1}$ & 130
35	29	2.47	131
46	38	2.40	13 $\bar{2}$
27	22	2.26	040
22	18	2.22	220
37	31	2.15	13 $\bar{3}$ & 041
22	18	2.03	202
74	62	2.00	005
19	16	1.96	133
43	36	1.66	151 & 11 $\bar{6}$
35	29	1.64	204
71	59	1.50	060

Table 2: XRD powder data of illite from Visé borehole V1b, 269m.

4.1 Major element geochemistry

The rock compositions are plotted in the classical TAS (Total Alkalis vs. Silica) diagram (Fig. 2) of Le Maître *et al.* (1989). The scattering of points covers a wide range of silica and total alkali contents from 51% to 82% SiO₂,

and from 3% to 13% Na₂O+K₂O, and, consequently, the rocks vary from supersaturated rhyolites to undersaturated phonolites. This approach has obviously little relevance.

We have chosen to use another chemographic representation, the Eskola ACF and AKF projections, which are widely used in metamorphic petrology (e.g. Winkler, 1979; Bucher & Frey, 1994). This representation permits to compare the chemical composition of a rock to common rock-forming minerals, and has the advantage of ignoring the quartz content of the rock, whose role is usually to dilute the other minerals contents (Figs 3-4). We have slightly modified the nature of the poles of the ternary diagrams to adapt them to our rocks. In the A component in both diagrams, we add Fe₂O₃ to Al₂O₃ (mol%) (assuming that all the Fe is ferric) and we subtract K₂O+Na₂O (mol%) (in order to plot K-feldspar and albite at the corner of the triangle). The K component is K₂O+Na₂O (mol%) and the F component is MgO (mol%). Because the anorthite content is negligible in the plagioclase of acidic rocks, we legitimately assume here that Ca is entirely in the form of calcite. Thus the C component is the CaO (mol%).

The AKF projection (Fig. 3) clearly shows that a series of illitic rocks (open triangles) plots on the muscovite-phengite tie line, close to the muscovite (sericite) composition. The illite composition (analysis n°28 in Table 1), when plotted in the AKF projection (Fig. 3B), remarkably coincides with the group of rocks previously defined. When these compositions are plotted in an Al₂O₃ vs. SiO₂ diagram (Fig. 5), they fall on a straight line linking quartz and the illitic group, which confirms that these rocks are essentially made up of two minerals, quartz and illite.

A second group of rocks in the AKF diagram (circles in Fig. 3) plots in an area between the feldspar pole and illite, and corresponds to less altered felsic material. The fact that some of the points are close to the point representative of the Bishop tuff rhyolites begs the question of possible preserved rhyolite compositions. The Na₂O vs. SiO₂, and K₂O vs. SiO₂ diagrams of Fig. 6 however show that the alkali contents are widely dispersed, thus demonstrating the high mobility of these elements in the metasomatic alteration of the rocks. Only 2 samples (n°20 and 26) have alkali contents similar to Bishop tuff rhyolite and might correspond to the least transformed original rhyolites, but in the ACF projection (Fig. 4) they are depleted in CaO compared to the Bishop tuff. In this projection it is clear that the second group of points is also widely dispersed: it extends towards the CF side of the ternary diagram, which means that they contain carbonates in their mineral assemblage. Two rocks of that group (n°2 and 14) are particularly rich in CaO (>12% CaO) and n°2 also contains 7% MgO.

It can be concluded from this chemographic approach that the Visé igneous rocks are characterized by the following paragenesis: quartz + illite ± carbonate ± relics of feldspars. Some sulphides (not accounted for by this type of projection and not systematically analysed) are also present. This type of mineral association characterises, in the Russian literature on metasomatism, rocks called berezite, which originate through replacement of granitic material and result from

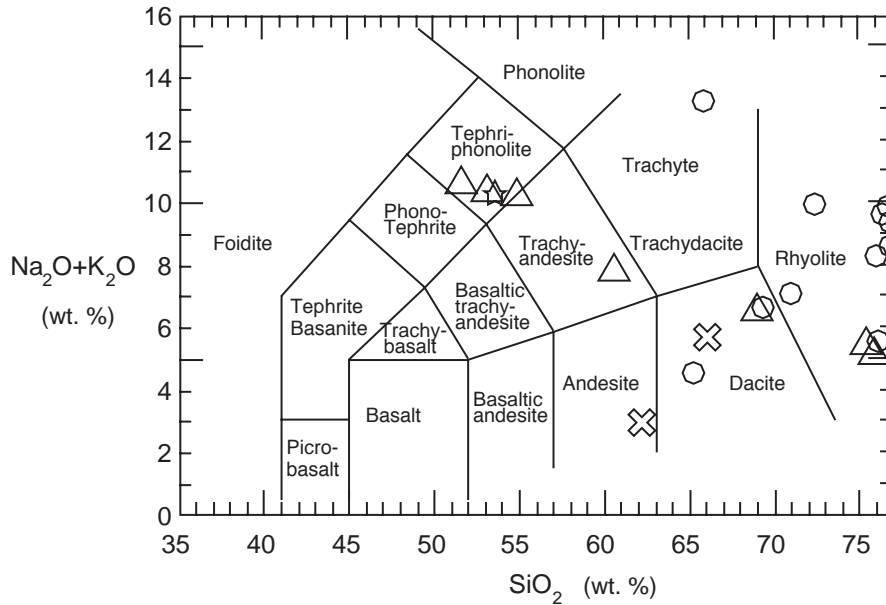


Fig. 2 : TAS (Total alkalis vs. Silica) diagram of Le Maître *et al.* (1989). Legend : see Fig.3.

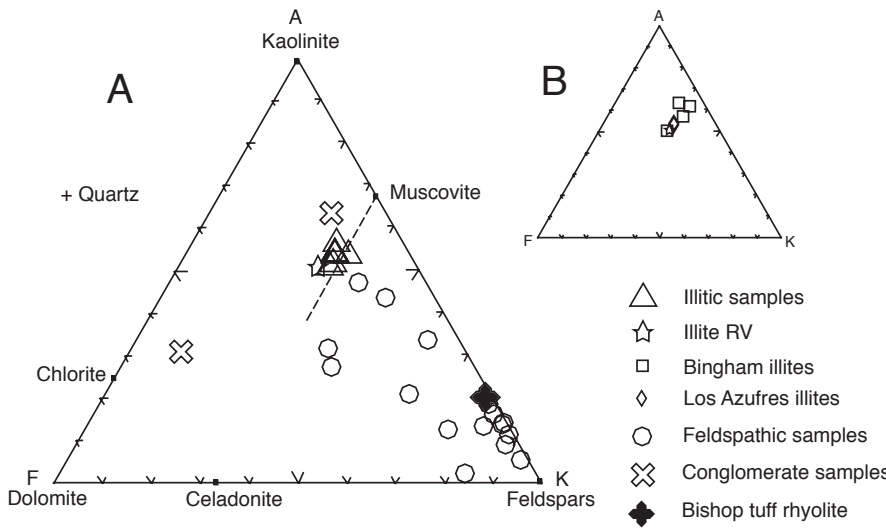


Fig. 3 : A. Chemical compositions of the Visé borehole samples projected in A (Al₂O₃+Fe₂O₃-Na₂O-K₂O) - K (K₂O+Na₂O) - F (MgO) diagram. B. Chemical compositions of illites (see Table 3).

	K	Na	Ca	IC ⁽¹⁾	Si	Ti	^{IV} Al	^{VI} Al	Mg	Fe	⁽²⁾ R ²⁺	K+ IFe-Mgl	T(°C) ⁽³⁾
<i>Visé borehole</i>													
RV	0,83	0,01	0,01	0,85	3,41	0,03	0,56	1,57	0,30	0,08	0,38	1,05	313
<i>Los Azufres</i>													
LA (6)	0,84	0,01	0,00	0,85	3,41	0,00	0,60	1,61	0,26	0,18	0,44	0,92	277
LA(7)	0,87	0,01	0,00	0,88	3,44	0,00	0,56	1,53	0,26	0,25	0,51	0,88	267
<i>Bingham</i>													
2-4	0,89	0,06	0,01	0,96	3,10	0,01	0,89	1,61	0,37	0,17	0,54	1,09	324
2-6	0,88	0,04	0,00	0,92	3,24	0,01	0,76	1,73	0,25	0,06	0,31	1,07	318
53-4	0,70	0,01	0,01	0,72	3,41	0,00	0,58	1,85	0,14	0,00	0,14	0,84	257
53-7	0,90	0,06	0,00	0,96	3,06	0,03	0,91	1,85	0,10	0,09	0,19	0,91	275

(1) IC = interlayer cations
 (2) R²⁺ = total number of divalent cations in the octahedral site
 (3) T(°C) = 267.95x + 31.50 where x= K+IFe-Mgl from Battaglia (2004)

Table 3: Structural formulae of illite (based on 11 oxygens) from Visé borehole compared to selected microprobe analyses of illites from the phyllic alteration of the Bingham porphyry-copper (from Parry *et al.*, 2002) and of the Los Azufres, Micoacan State, Mexico (Battaglia, 2004), and application of the illite geothermometer of Battaglia (2004).

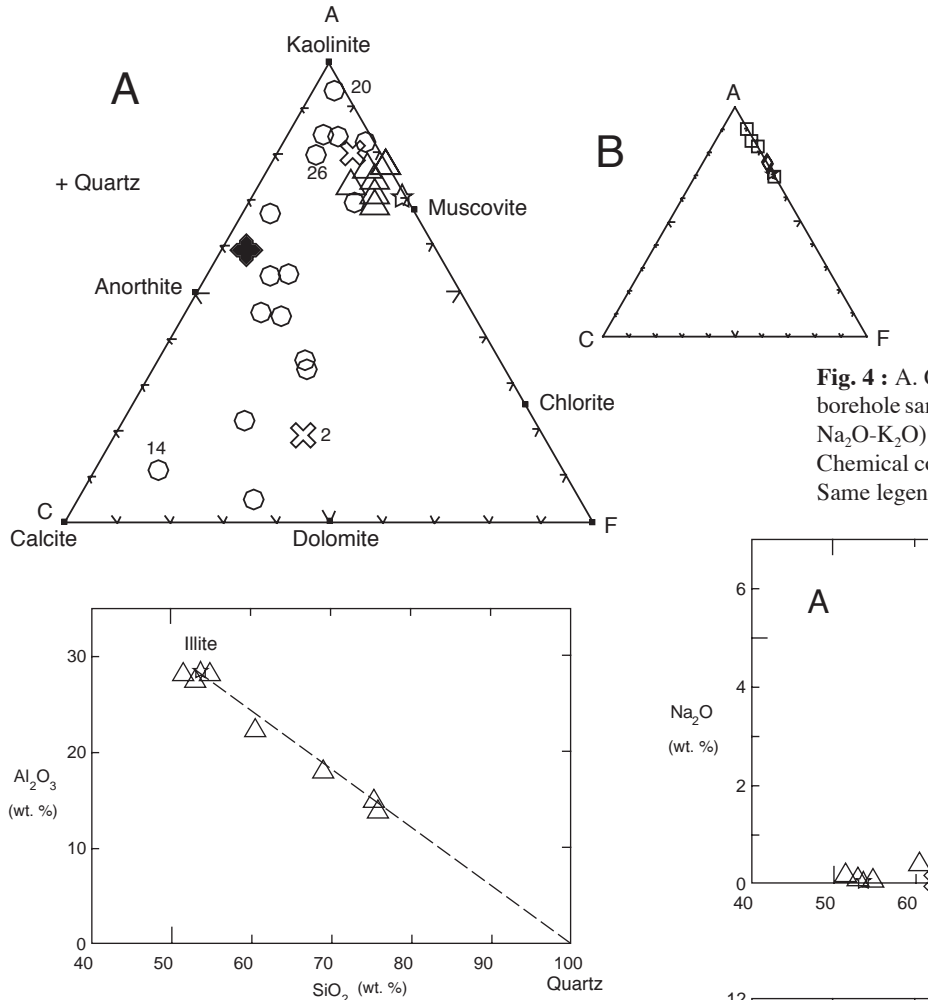


Fig. 4 : A. Chemical compositions of the Visé borehole samples projected in A ($\text{Al}_2\text{O}_3+\text{Fe}_2\text{O}_3$ - $\text{Na}_2\text{O}-\text{K}_2\text{O}$) - C (CaO) - F (MgO) diagram. B. Chemical compositions of illites (see Table 3). Same legend as in Fig. 3.

Fig. 5 : Al_2O_3 vs. SiO_2 in illitic samples of the Visé felsic rock. Same legend as in Fig. 3.

acidic metasomatism under the conditions of feldspar and kaolinite instability (Zharikov *et al.*, 1998).

4.2 Trace element geochemistry

4.2.1 Immobile elements

In metasomatic processes, some elements, considered mobile, can leave or enter the chemically open system. Some others, which remain inside the system, are called immobile or inert elements. In the present case it emerges from what we have shown that Na, K, Ca and Si are mobile elements. We can anticipate that Rb and Sr, which are diadochic with the alkalis also belong to that category. The status of the other elements is ambiguous. Even if they stay within the system, the original contents of the immobile elements are modified by dilution/concentration processes in response to the mobile element behaviour. The intensity of the metasomatic transformation can also change the character of an element, from inert in low grade conditions to mobile in higher grade conditions. There is, however, a straightforward method to assess the immobile characters of elements by considering the ratios of immobile elements which do not form diadochic pairs. The ratios

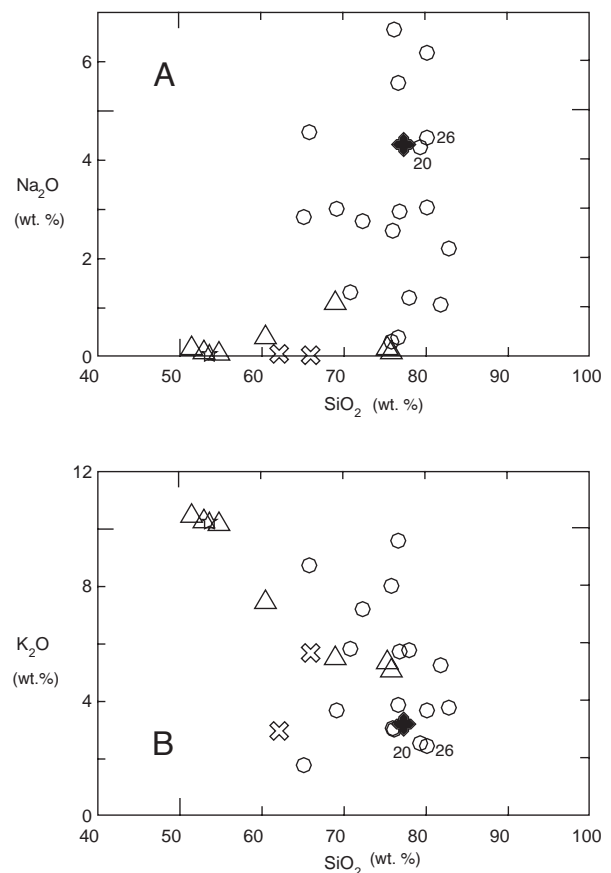


Fig. 6 : Mobile elements in the Visé felsic rock. A : Na_2O vs. SiO_2 ; B : K_2O vs. SiO_2 . All contents in wt%. Same legend as in Fig. 3. Samples with number are particularly discussed in the text.

indeed remain constant in the system however intense the metasomatic alteration.

We have plotted in Fig. 7 the TiO_2 , Y, Th, and Nb contents against Zr content. Where the ratio of two elements is constant, their contents plot on a straight line. Except for the samples 1 and 2, which belong to the conglomeratic rocks above the unconformity, the samples from the Visé igneous rocks tend to define straight arrays in all diagrams. The relationship is somewhat less well defined in the Y vs. Zr diagram,

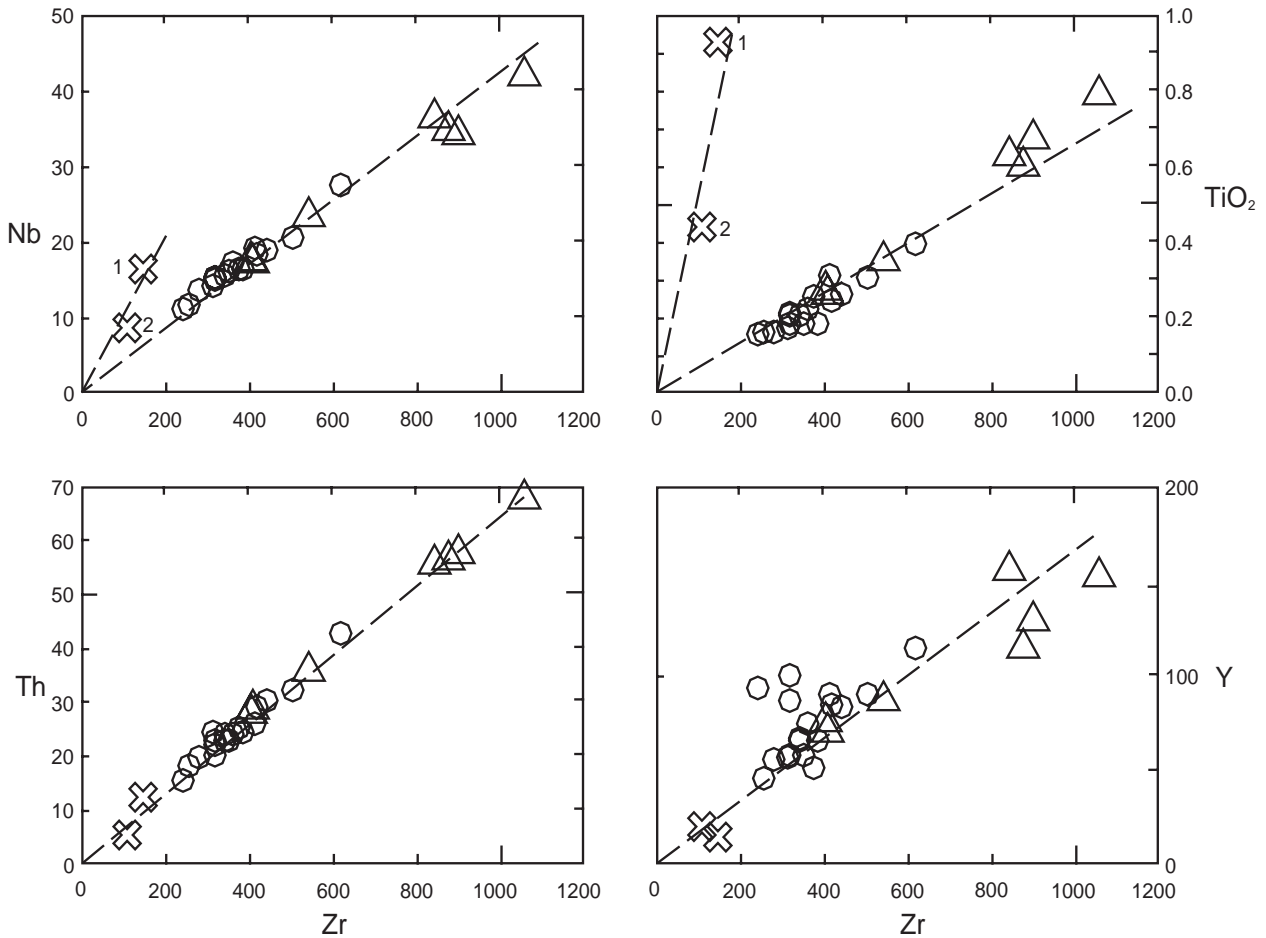


Fig. 7 : Immobile elements in the Visé felsic rocks. Nb, Th, Y and TiO₂ vs. Zr. Trace elements in ppm; major element in wt%. Same legend as in Fig. 3.

implying that Y might have been somewhat mobile in a few samples. On the whole it can be considered that these elements have been immobile in the alteration process of the Visé igneous rock. In the Nb vs. Zr and TiO₂ vs. Zr diagrams the 2 samples from the conglomeratic rocks above the unconformity grossly define linear

arrays passing through the origins. They can thus also be immobile but with different Nb/Zr and TiO₂/Zr ratios.

Having identified the immobile elements in the metasomatic alteration, we can use them to identify the nature of the protolith in the discrimination diagram of Winchester & Floyd (1977) (Fig. 8). It is obvious that

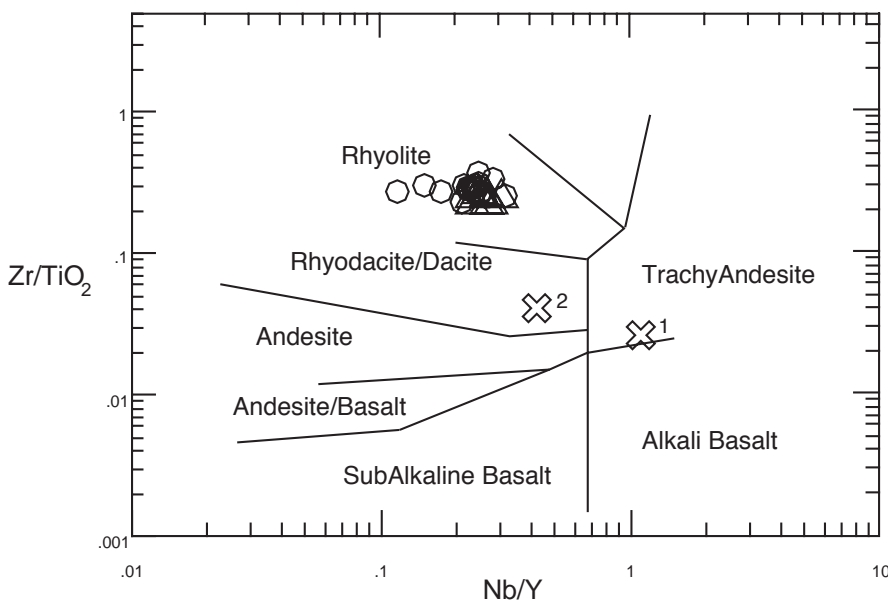


Fig. 8 : Zr/TiO₂ vs. Nb/Y diagram of Winchester & Floyd (1977). Same legend as in Fig. 3.

Analysis #	9	14	17	21
Sample	V1.19	V1b.8	V1b33	V1b.74
concentrations in parts per million (ppm)				
Ba	799	115	1394	208
Hf	9	8	16	29
Ta	0,9	0,7	2,3	3,2
La	63	44	86	132
Ce	136	104	179	285
Pr	16	13	21	33
Nd	64	53	77	127
Sm	12	14	14	24
Eu	1,1	1,5	1,4	2,0
Gd	13	17	12	18
Tb	2,2	3,0	1,8	2,7
Dy	13	17	12	17
Ho	2,9	3,2	2,8	4,2
Er	9	9	9	14
Tm	1,2	1,1	1,4	2,1
Yb	8	8	11	16
Lu	1,3	1,0	1,8	2,4
Th/Yb	2,6	2,1	2,9	3,6
Ta/Yb	0,1	0,1	0,2	0,2

Table 4: Trace element composition of selected samples from the Visé boreholes.

the Visé igneous rock compositions plot as a well-grouped cluster in the rhyolite field. We can thus deduce that the protolith of the Visé igneous rock was effectively a rhyolite.

Figure 8 also shows that the conglomeratic rocks plot in the fields of trachy-andesite and rhyodacite-andesite. This shows that the volcanic component of these rocks has a different composition than the Visé rhyolite, but has still a calc-alkaline character.

4.2.2 Rare Earth elements

Rare Earth elements (REE) have been determined in 4 selected samples (Table 4). Their chondrite-normalized distributions are shown in Fig. 9. Three out of four samples typically display similar spectra with $[La/Yb]_N$ ratios between 5.1 and 6.0 and large negative Eu anomalies ($Eu/Eu^* = 0.26-0.33$), typical of evolved magmas. The spectra are remarkably parallel, particularly between sample n°17 (with a composition in the range of rhyolites) and sample n°21 (highly altered into berezite). This shows that the alteration process has not significantly modified the REE distribution, thus preserving the original ratios. The REE can thus be considered immobile in the alteration process. A small difference can be observed with sample n° 14, rich in carbonate, which shows a slightly lower $[La/Yb]_N$ ratio of 4.5. More data are needed, however, to ascertain the meaning of this difference, maybe in relation with the Pb-Zn carbonate fluids that have affected the area.

4.2.3 Multi-element diagrams

The rhyolite compositions have been normalized to the ocean ridge granite (ORG) of Pearce *et al.* (1984) and plotted in Fig. 10. The spectra are typical of evolved

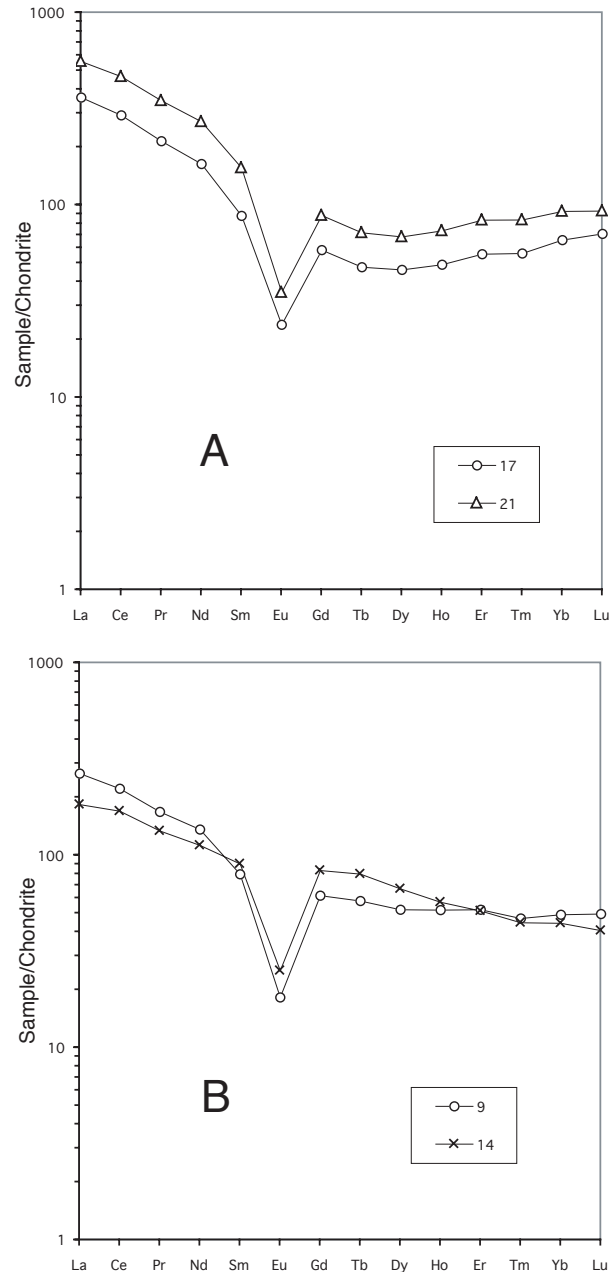


Fig. 9: Chondrite-normalised REE contents in Visé felsic rocks. A: Samples with different degrees of alteration; B: Sample 14, rich in carbonates, has a slightly lower $[La/Yb]_N$ ratio than common samples. Normalising values after Sun & McDonough (1989).

rocks, except for Rb and Ba which show large variations due to their mobile character. The distributions display a large negative anomaly of Nb and Ta in all samples, and a smaller negative anomaly of Zr and Hf in samples 9 and 14. The latter can be ascribed to zircon fractionation, and the former is typical of calc-alkaline magmas, produced in subduction zones (Thompson *et al.*, 1984) or by crustal melting in post-collisional settings (Liégeois, 1998). The high Th/Hf and Th/Ta ratios are typical of calc-alkaline rocks in the discrimination diagram of Wood *et al.* (1979) and the Th/Yb and Ta/Yb ratios plot in the continental margin calc-alkaline field of Pearce (1983). In the Nb vs. Y diagram of Pearce *et al.*

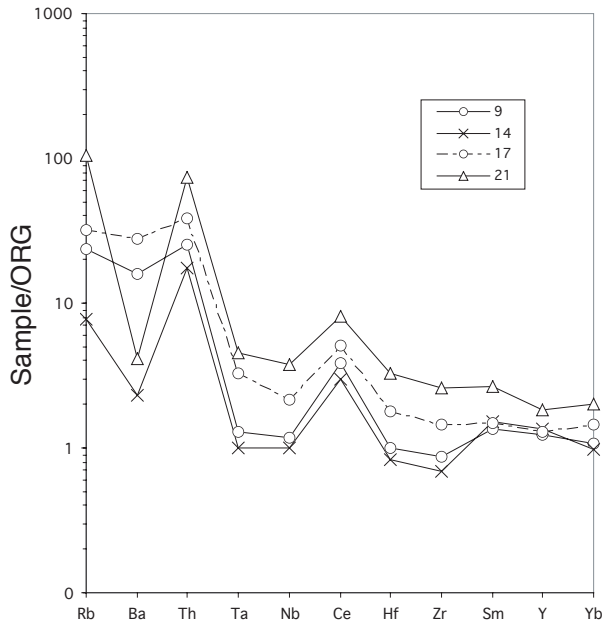


Fig. 10 : Multi-element diagram. Ocean Ridge Granite (ORG) normalised trace element contents after Pearce (1983)

(1984) the illitic samples plot in the within plate field (WPG on Fig. 11). The rhyolite could thus have been generated in an extensional post-collisional environment (Liégeois, 1998), as an alternative to the subduction process. It is conceivable that during the collision of Avalonia areas of localized extension could develop as the shape of Avalonia was adjusted to fit the continents it was colliding with (J.A. Winchester, pers. com.).

4.2.4 Uranium and Radon contents

U contents have been plotted versus the Zr content in Fig. 12A. It immediately emerges that, unlike Th, an immobile element, U does not show a linear relationship with Zr, and has to be considered mobile. U^{4+} has probably been mobilized in oxidizing conditions as the

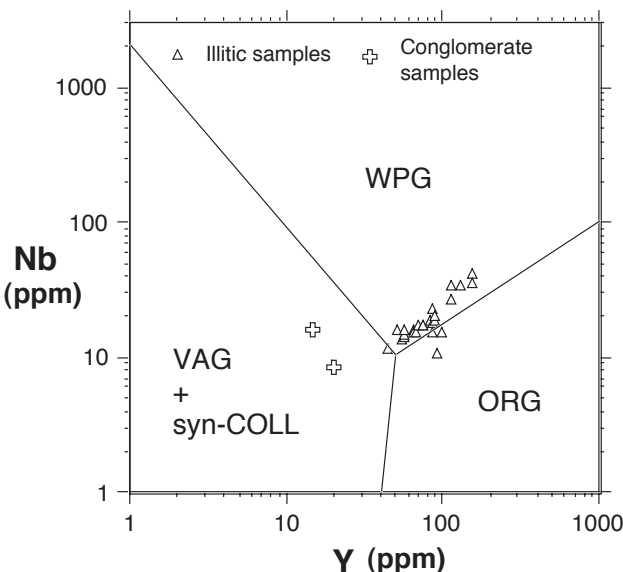


Fig. 11 : Nd vs. Y diagram of Pearce *et al.* (1984).

uranyl ion (UO_2^{2+}). Fig. 12B shows a gross correlation between U and Rn. This was to be expected since Rn is a decay product of U. A number of samples plot far above a line passing through the origin, which means that part of the U present in these samples does not produce Rn because it was contained into minerals that are closed to Rn escape, such as non-metamict zircon. It should be noted that the Rn values are somewhat higher than the values found in Belgian sedimentary pelitic rocks (Vanderschueren, in prep.).

4.2.5 Zinc: an indicator of mineralised carbonate veins

Zn shows large variations in the investigated samples (Fig. 13). Some samples can reach 250 ppm and contrast with average contents <25 ppm for the others. Since some of these samples, e.g. n°14, are very rich in CaO, this suggests a link between Zn and carbonate veins, which would reflect the influence of mineralising fluids of late Silurian to early Devonian age (Dewaele & Muechez, 2004) or of later age (Heijlen *et al.*, 2000).

5. Conditions and age of the metasomatic alteration

The Visé illite formula (Table 3) well agrees with published data (e.g. Battaglia, 2004) and particularly

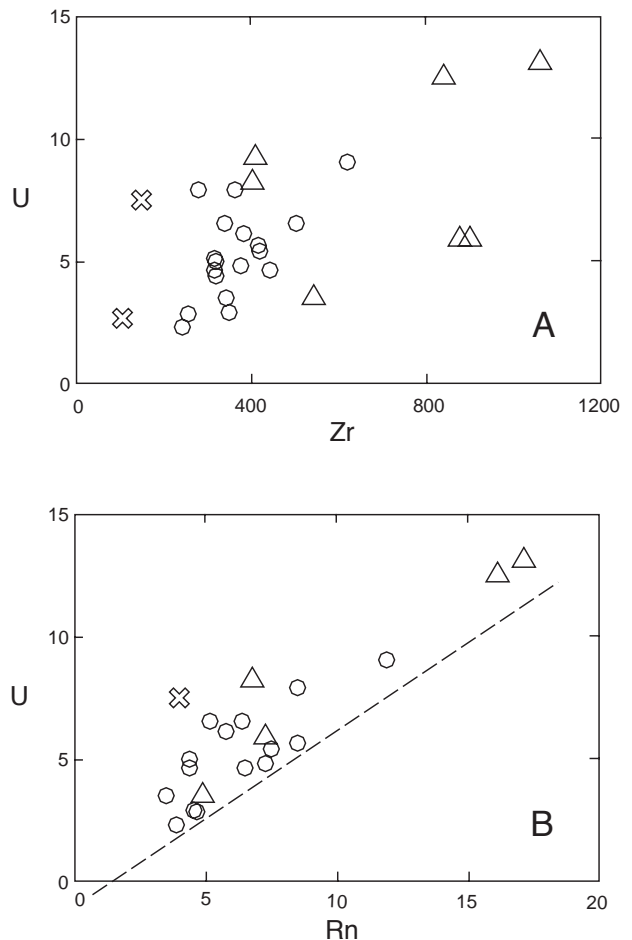


Fig. 12 : Radon diagrams. A : U (ppm) vs. Zr (ppm) in Visé felsic rocks. B : U (ppm) vs. Rn ($Bq/m^3.kg$) in selected samples from the Visé felsic rock.

with illite from the active geothermal system of the Pleistocene silicic volcanic (dacitic, rhyodacitic, and rhyolitic) centre of Los Azufres (Trans-Mexican volcanic, Dobson & Mahood, 1985). It is also close in composition to muscovite from the phyllic alteration of the Bingham porphyry copper deposit (Parry *et al.*, 2002). In the AKF projection (Fig. 3B), the compositions determined by microprobe analyses plot on the tie line between muscovite and illite and merge with the Visé illite composition. It is worth noting that the illite composition in Visé is less variable than in the Bingham phyllic zone. This points to more restricted conditions of formation than in Bingham. Battaglia (2004) has observed and quantified a relationship between the K, Fe and Mg contents in illite and the temperature of formation. Application of this geothermometer to the Visé illite (Table 3) suggests a temperature of formation of ca. 310°C. Table 3 also shows that, calculated with the same geothermometer, the temperatures of formation at Bingham and Los Azufres are constrained between 250° and 325°C. This interval of temperature is commonly accepted for this type of alteration in porphyry copper deposits (see the review by Parry *et al.*, 2002), based on fluid inclusion studies and the low percentage of expandable layers ("Ir" ratio) in illite. A somewhat larger temperature interval (250°-450°C) is suggested by Russian studies for beretization processes (Zharikov *et al.*, 1998).

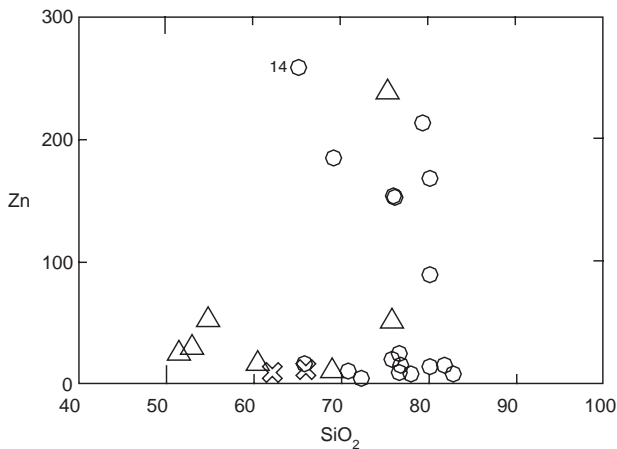


Fig. 13 : Zn (ppm) vs. SiO₂ (wt%) in the Visé felsic rock. Sample n°14 is particularly rich in CaO (15.12%).

The ages of emplacement of the Visé rhyolite and of its alteration are not known and may be different. Several episodes of brecciation are known in this area (Poty, 1991) and hydrothermal mineralizations up to Jurassic in age are conspicuous in eastern Belgium. We have observed an angular clast in a polygenic breccia (Plate 1, ph. F) which is not affected by the same type of transformation as the other clasts of the same rock: the feldspar phenocrysts are pseudomorphosed by sericitic material, but the « glassy » matrix of the rock is not illitised, in contrast with the other clasts. The plagioclase content and the embayed quartz suggest a dacitic composition, thus not very different in composition from a rhyolite and likely to have been affected by the same type of alteration. This strongly suggests that the alteration of the rhyolite took place before its brecciation

and incorporation into a pyroclastic flow. The hydrothermal alteration would thus have started in the deuteric stage of the magmatic evolution and be sub-contemporaneous with the volcanic event. An ³⁹Ar/⁴⁰Ar dating of the illite would thus give a magmatic age.

6. Conclusions

The Visé felsic rock is commonly auto-brecciated and very rarely of pyroclastic origin. Flow structures are conspicuous and, microscopically, devitrification microstructures with evidence of illitisation, carbonation and silicification, are very well developed. Occurrence of non-illitized clast in an illitised pyroclastic flow points to a late magmatic alteration process.

The original quartzo-feldspathic composition of the rock has been deeply metasomatised, with progressive transformation of the feldspars into a simple association : quartz + illite ± carbonate + sulphide (beresite or phyllic alteration) at temperature ca. 310°C.

Constant ratios of elements such as REE, Y, Nb, Zr, Th, and Ti attest the immobile character of these elements and permit the determination of the protolith name (rhyolite), magmatic series (calc-alkaline trend) and geodynamic setting. Radon contents are grossly proportional to U contents.

The Visé rhyolite, showing calc-alkaline affinities, most probably belongs to the Ordovician-Silurian magmatic arc and its eastern concealed prolongation. A post-collisional setting corresponding to local areas of extension is preferred to simple subduction.

The volcanic components of the polygenic conglomerates above the unconformity (Lower Devonian age) also show the characteristics of a calc-alkaline series, but with a different source signature. They could thus belong to a different type of volcanism and originate in another volcanic rock, Ordovician-Silurian or Devonian in age.

7. Acknowledgements

The authors are greatly indebted to the Geological Survey of Belgium (Ir. G. Vandenven) for donating samples of the Visé boreholes. The reviews of J. Verkaeren and J.A. Winchester were greatly appreciated. G. Bologne has helped with the chemical analyses at the « Collectif Interuniversitaire de Géochimie Instrumentale » (University of Liège).

Appendix

Methodology and methods

Whole rock analyses were performed by XRF on an ARL 9400 XP spectrometer. The major elements were analysed on Li tetra- and metaborate glass discs (Fluore-X 65®), on calcinated powder with matrix corrections following the Traill-Lachance algorithm. Trace elements (Sr, Rb, Nb, Zr, Y, U, Th, Pb, Ga, Ni, Zn, Co and Cu) were measured on pressed pellets and corrected for matrix effects by Compton peak monitoring. Selected samples were analysed for REE, Hf, Ta and Ba by ICP-MS on a VG Elemental Plasma Quad PQ2 after

alkali fusion following the method described in (Vander Auwera *et al.*, 1998).

Radon was measured with a ALPHAGUARD Professional Radon Monitor (Genitron Instruments). A 50g sample of crushed rock is enclosed during ca. 4 days (Rn half-life) in a 3/8-liter cell, itself contained with 50 gr of sample in a 3/4-liter receptacle (playing a guard role against leakage). The cell is connected through a circulation pump to the monitor, which measures the Rn level in close circuit during 35 m.

X-ray diffraction (XRD) studies were performed on a Philips PW1730 spectrometer, with Cu-anticathod and Ni-filter, working at 30kV, 30mA. Determinations were carried out on bulk sample (<250 μ m disoriented powders) and on <2 μ m-fraction (extracted after crushing and sedimentation). For each sample qualitative and semi-quantitative determinations of clay and non-clay minerals were carried out. The clay mineral composition was determined in oriented specimens (N: air-dried, EG: glycolated and Q: heated 4h at 500°C).

References

- ANDRÉ, L., 1991. Caledonian magmatism. In André, L., Herbosch, A., Vanguetaine, M. & Verniers, J. (ed.) *Guidebook to the excursion on the stratigraphy and magmatic rocks of the Brabant Massif*, Annales Société géologique de Belgique, 283-323.
- ANDRÉ, L., DEUTSCH, S. & HERTOGEN, J., 1986. Trace-element and Nd isotopes in shales as indexes of provenance and crustal growth: the early paleozoic from the Brabant massif (Belgium). *57*, 101-115.
- ANDRÉ, L., HERTOGEN, J. & DEUTSCH, S., 1986. Ordovician-Silurian magmatic provinces in Belgium and the Caledonian orogeny in middle Europe. *Geology* 14, 879-882.
- BATTAGLIA, S., 2004. Variations in the chemical composition of illite from five geothermal fields: a possible geothermometer. *Clay Minerals* 39, 501-510.
- BUCHER, K. & FREY, M., 1994. *Petrogenesis of metamorphic rocks*. Springer, Heidelberg, 318 p.
- CHACKSFIELD, B.C., DE VOS, W., D'HOOGHE, L., DUSAR, M., LEE, M.K., POITEVIN, C., ROYLES, C.P. & VERNIERS, J., 1993. A new look at Belgian aeromagmatic and gravity data through image-based display and integrated modelling techniques. *Geological Magazine* 130, 583-591.
- DE VOS, W., VERNIERS, J., HERBOSCH, A. & VANGUESTAINE, M., 1993. A new geological map of the Brabant Massif, Belgium. *Geological Magazine* 130, 605-611.
- DEWAELE, S. & MUCHEZ, P., 2004. Alteration, mineralisation and fluid flow characteristics in the Bierghes sill, Anglo-Brabant fold belt, Belgium. *Geologica Belgica* 7,
- DOBSON, P.F. & MAHOOD, G.A., 1985. Volcanic stratigraphy of the Los Azufres geothermal area, Mexico. *Journal of Volcanic and Geothermal Research* 25, 273-287.
- ESQUEVIN, J., 1969. Influence de la composition chimique des illites sur la cristallinité. *Bulletin Centre de Recherches de Pau* 3, 147-154.
- GOEMAERE, E. & VANDENVEN, G., 1989. The Visé boreholes (abstract). *International Meeting Caledonides Midlands Brabant Massif*, 27.
- HEIJLEN, W., MUCHEZ, P., BANKS, D. & NIELSEN, P., 2000. Origin and geochemical evolution of synsedimentary, syn- and post-tectonic high-salinity fluids at the variscan thrust front in Belgium. *Journal of Geochemical Exploration* 69-70, 149-152.
- HILDRETH, W., 1981. Gradients in silicic magma chambers: implications for lithospheric magmatism. *J. Geophys. Res.* 86, 10153-10192.
- LIÉGEOIS, J.P., 1998. Preface - Some words on the post-collisional magmatism. *Lithos* 45, XV-XVII.
- MCPHIE, J., DOYLE, M. & ALLEN, R., 1993. *Volcanic textures*. CODES, Hobart, 196 p.
- PARRY, W.T., JASUMBACK, M. & WILSON, P.N., 2002. Clay mineralogy of phyllic and intermediate argillic alteration at Bingham, Utah. *Econ. Geol.* 97, 221-239.
- PEARCE, J.A., 1983. Role of sub-continental lithosphere in magma genesis at active continental margins. In Hawkesworth, C.L. & Norry, M.J. (eds) *Continental basalts and mantle xenoliths*, Shiva, Nantwich, 230-249.
- PEARCE, J.A., HARRIS, N.B.W. & TINDLE, A.G., 1984. Trace element discrimination diagrams for the tectonic interpretation of granitic rocks. *J. Petrol.* 25, 956-984.
- PHARAOH, T.C., BREWER, T.S. & WEBB, P.C., 1993. Subduction-related magmatism of late Ordovician age in eastern England. *Geological Magazine* 130, 647-656.
- POTY, E., 1991. Tectonique de blocs dans le prolongement oriental du massif de Brabant. *Annales Société géologique de Belgique* 114, 265-275.
- SUN, S.S. & MCDONOUGH, W.F., 1989. Chemical and isotopic systematics of oceanic basalts: implications for mantle composition and processes. In Saunders, A.D. & Norry, M.J. (eds) *Magmatism in ocean basins*, Geol. Soc. London Spec. Pub., 313-345.
- THOMPSON, R.N., MORRISON, M.A., HENDRY, G.L. & PARRY, S.J., 1984. An assesment of the relative roles of crust and mantle in magma genesis: an elemental approach. *A310*, 549-590.
- VAN GROOTEL, G., VERNIERS, J., GEERKENS, B., LADURON, D., VERHAREN, M., HERTOGEN, J. & DE VOS, W., 1997. Timing of magmatism, foreland basin development, metamorphism and inversion in the Anglo-Brabant fold belt. *Geological Magazine* 134, 607-616.
- VANDERAUWERA, J., BOLOGNE, G., ROELANDTS, I. & DUCHESNE, J.C., 1998. Inductively coupled plasma-mass spectrometry (ICP-MS) analysis of silicate rocks and minerals. *Geologica Belgica* 1, 49-53.
- VERNIERS, J., PHARAOH, T.C., ANDRÉ, L., DEBACKER, T.N., DE VOS, W., EVERAERTS, M., HERBOSCH, A., SAMUELSON, J., SINTUBIN, M. & VECOLI, M., 2002. The Cambrian to mid Devonian basin development and deformation history of eastern Avalonia, east of the Midlands Microcraton: new data and a review. In Winchester, J.A., Pharaoh, T.C. & Verniers, J. (eds) *Paleozoic amalgamation of Central Europe*, Geological Society of London, Special Publication, 47-93.

VERNON, R.H., 2004. *A practical guide to rock microstructure*. Cambridge University Press, Cambridge, 594 p.

WINCHESTER, J.A. & FLOYD, P.A., 1977. Geochemical determination of different magma series and their differentiation products using immobile elements. *Chem. Geol.* 20, 325-343.

WINKLER, H.G.F., 1979. *Petrogenesis of metamorphic rocks*. Springer, Heidelberg, 348 p.

WOOD, D.A., JORON, J.L. & TREUIL, M., 1979. A re-appraisal of the use of trace elements to classify and discriminate between magma series erupted in different tectonic settings. *Earth and Planetary Science Letters* 45, 326-336.

ZHARIKOV, V.A., RUSINOV, V.L., MARAKISHEV, A.A., ZARAIKII, G.P., OMEL'YANENKO, B.I., PERTSEV, N.N., RASS, I.T., ANDREEVA, O.V., ABRAMOV, S.S. & PODLESSKII, K.V., 1998. *Metasomatism and metasomatic rocks (In Russian)*. Scientific World, Moscow, 492 p.

Plate caption

- A. Brecciated felsic rock possibly due to autobrecciation processes, all fragments being of the same nature. Sample V1.42.
- B. Convolute structure (flow folds) in a banded pink felsic rock. Sample V1b.60.
- C. Partly illitised flow banding. In the upper right part of the microphoto, flow bands are deflected around silicic clasts due to ductile deformation during flowage. In the lower left part, illite has developed mimetically with the flow banding. Thin section. Crossed nicols. Sample V1b.43.
- D. Completely illitized sample. The orientation of the illite is probably mimetic with an original banded structure. The opaque mineral is pyrite. Thin section. Crossed nicols. Sample V1b.06.
- E. Various types of recrystallised spherulitic quartz. Note, at the centre of the picture, the monocrystalline (undeformed) rounded crystal, rimmed by radial quartz fibres. Thin section. Crossed nicols. Sample V1b.61.
- F. Porphyritic structure of a clast in the polymict breccia. Euhedral feldspar crystals, completely altered into sericitic material, and an embayed quartz crystal are embedded in a « glassy » groundmass. Thin section. Sample V1.15 (G).
- G. Spherulitic quartz. The quartzo-feldspathic matrix is partly illitised. Thin section. Crossed nicols. Sample V1.16 (G).
- H. Fibrous, spherulitic feldspar and quartz that have grown on quartz phenocrysts. Thin section. Crossed nicols. Sample V1b.34.

